

# Variability in Soil Erodibility Parameters of Tigris Riverbanks Using Linear and Non-Linear Models

Abdul-Sahib T. Al-Madhhachi

Department of Environmental Engineering

University of Mustansiriyah

[abdu@okstate.edu](mailto:abdu@okstate.edu);

[a.t.almadhhachi@uomustansiriyah.edu.iq](mailto:a.t.almadhhachi@uomustansiriyah.edu.iq)

## Abstract

Most researches have predicted soil erosion of cohesive riverbanks using linear (excess shear stress model) and non-linear (Wilson model) models based on two soil parameters (detachment coefficient,  $k_d$ , and critical shear stress,  $\tau_c$ ) of the linear model and two soil mechanistic parameters (mechanistic detachment parameter,  $b_0$ , and threshold parameter,  $b_1$ ) of the non-linear model. The goal of this research was to quantify the soil erodibility parameters of Tigris Riverbanks on Nu'maniyah-Kut Barrage reach using linear and non-linear models through the model parameters at three different water contents: dry side, optimum side, and wet side of water contents. Soil samples were collected from three locations south of Baghdad city on Nu'maniyah-Kut Barrage reach of Tigris Riverbanks. Six soil samples acquired from these sites were laboratory tests achieved using a miniature version of Jet Erosion Test device ("mini" JET) to determine the erodibility parameters of both linear and non-linear models. Blaisdell solution (BL) and scour depth solution (SD) were applied to determine ( $k_d$  and  $\tau_c$ ) of linear model from JETs data. Physical soil characteristics; including bulk density, particle size distribution (sand%, silt%, and clay%), average particle size ( $D_{50}$ ), and angle of repose were reported for six samples acquired from the three sites. The results showed lower value of  $k_d$  of toe in compared with bank side for some specific sites as observed for both BL and SD solutions of excess shear stress model especially at wet side of water content. No general pattern of  $\tau_c$  related to different water content were observed. The parameters ( $b_0$  and  $b_1$ ) of non-linear model have the same behavior of linear model parameters ( $k_d$  and  $\tau_c$ ), but with different magnitude related to different water contents, respectively.

**Keywords:** Linear model, Non-linear model, Soil erodibility parameters, Tigris Riverbanks, JETs

## 1 Introduction

Riverbanks erosion is significant challenge for many scientists and engineers. Estimating riverbank detachment rates is significant due to that detachment rate is known as one of the main

nonpoint sources of deposit pollution of rivers [1, 2]. Therefore, measuring sediment detachment is one of the most significant problems for estimating riverbanks sediment loads.

Erosion models are engaged to predict rates of detachment caused by water processes within a riverbank. Classically the detachment rate of cohesive riverbanks is predicted using linear and non-linear models. The linear model (excess shear stress) is widely employed to determine detachment rate depending on two empirical soil parameters [3, 4, 5, 6]: detachment coefficient,  $k_d$  ( $\text{cm}^3/\text{N.s}$ ), and critical shear stress,  $\tau_c$  (Pa). A different model with more fundamentally based, mechanistic detachment model was presented by Wilson (1993a, 1993b) [7, 8]. A general outline for studying soil particle and fluid properties and their influence on cohesive and non-cohesive soil erodibility were presented by Wilson (1993a, 1993b) [7, 8]. The detachment mechanistic model refers to Wilson model (non-linear model). Two dimensional demonstrations of soil particles to determine soil erodibility was developed in Wilson model based on two mechanistic soil parameters: mechanistic detachment parameter,  $b_0$ , and threshold parameter,  $b_1$ .

Soil texture, soil structure, unit weight of soil, soil moisture content, water chemistry, and other factors can influence the erodibility parameters of cohesive soils [9, 5]. A correlation between soil physical and detachment parameters from the linear model (excess shear stress model) were developed [10, 11]. Inverse relationships were suggested in pervious and recent researches in order to determine  $k_d$  as a function of  $\tau_c$  as well as to  $b_0$  as a function of  $b_1$  for cohesive soils [12, 13, 14, 15, 16, 17, 18]. More researches are needed to verify these relationships in a wide variety of cohesive soils. These relationships are very useful and may be incorporated in many widely used erosion models; such as SWAT (Soil and Water Assessment), CONCEPTS, (Conservational Channel Evolution and Pollutant Transport Systems), WEPP (Water Erosion Prediction Project), and BSTEM (the Bank Stability and Toe Erosion Model) [1, 19, 20, 21].

Sediment detachment models (linear and non-linear models) are usually utilized in the laboratory using various experimental methods. Jet Erosion Test (JET) device is a novel method to

derive detachment parameters in the field as well as in the laboratory. Two versions of JET devices were recently developed; the original JET device [4], and the “mini” JET device [5, 6]. The “mini” JET device is easy to handle and setup in the field as well as in the laboratory comparing to original JET device. The original JET is bigger, heavier, and required more water compared to “mini” JET. Equivalent erosion parameters of linear model were provided by Al-Madhhachi et al. (2013a) [5] between “mini” JET versus original JET under controlled laboratory setup. Both original and “mini” JETs were verified with flume data tests as reported in Al-Madhhachi et al. (2013b) [6] from deriving both linear model and non-linear model parameters ( $k_d$ ,  $\tau_c$ ,  $b_0$ , and  $b_1$ ). Twenty “mini” JETs under controlled laboratory conditions were conducted by Khanal et al. (2016) [22] on two soil types of contrasting texture to investigate the variability of “mini” JET device on estimating soil erodibility parameters. Khanal et al. (2016) [22] recommended that at high pressure head, the initial time interval should be taken at least 0.5 minute and a termination time interval should be at least 5 minutes for less erodible soils.

Daly et al. (2015a) [15] performed the “mini” JET in at riverbanks of the Illinois River in northeast of Oklahoma to determine the erodibility parameters. At a river basin scale, they investigated the variability or uniformity in the erodibility parameters. Daly et al. (2015a) [15] was developed relationships between the soil texture and the erodibility parameters to predict the  $k_d$  - $\tau_c$  and  $b_0$ - $b_1$  relationships. Daly et al. (2015b) [16] utilized BSTEM to evaluate bank retreat rates compared to in situ bank retreat measurements due to streambank erosion and failures. Daly et al. (2016) [17] investigated the variations of erodibility parameters in site-scale of three different watersheds in Oklahoma. They performed a total of 74 JETs at these watersheds with variation of erodibility parameters up to three orders of magnitude at these watersheds. Daly et al. (2016) [17] investigated that there was no strong correlation variables across these watersheds were observed between erodibility parameters and soil physical properties. These pervious researches were performed on specific field water content sites and did not count the variability in soil detachment parameters at different water contents.

In this research, a case study of Tigris Riverbanks upstream of Kut Barrage, southern Baghdad city, was investigated to inspect the variability of soil erodibility parameters at three different sites and at different water contents. The aim of this research was to examine the variability of detachment parameters using linear model (excess shear stress model) and non-linear model (Wilson model) of Tigris Riverbanks upstream of

Kut Barrage at three different water contents: dry side, optimum side, and wet side of water contents. A “mini” JET device was utilized to derive the detachment model parameters ( $k_d$  and  $\tau_c$ ) of linear model and ( $b_0$  and  $b_1$ ) of non-linear model under controlled laboratory setups. Examination of correlations between soil characteristics and the derived erosion parameters as well as to site properties was performed.

## 2 Methods and Material

### 2.1 Study Area and Data Collection

This study focused on the Tigris Riverbanks between Nu'maniyah city and Kut Barrage, southern Baghdad, with a reach of 73km long as shown in Figure 1. The reach has some sand bars and vegetation on banks and in the main channel of Tigris River. There are some main channels branching out from the Tigris River in this reach such as AL Husiniya channel, Ahwar channel, Al Battar channel, Dalmage channel, Al Mazag channel, Al Suwada channel, Al Gharaf River, and Al Dejila channel [23]. The composite Tigris Riverbanks include silty sand at the top layer and silty clay at the bottom layer and toe. Tigris Riverbanks ranged from 1 to 6 m in height with a cohesive soil at top and bottom layers. The cohesive top layer was typically 0.5 to 4m thick and the bottom layer ranged from 4 to 6m. Both cohesive layers of Tigris Riverbanks were generally classified as silty sand at the top layer and silty clay at the bottom.



**Figure 1:** Locations of three sites of Nu'maniyah-Kut Barrage reach of Tigris Riverbanks.

Tigris Riverbanks reach data were acquired at three sites within the reach of Nu'maniyah-Kut Barrage (Figure 1). The required sites were selected based on more critical banks, safety issue, and easy to access. Six soil samples were acquired from the three sites at the bank and toe of each site. Disturbed soil samples were brought back to the Soil Laboratory, Engineering College, Mustansiriyah University, where sieve analysis and hydrometer tests were performed to quantify the particle size distributions, geotechnical parameters (soil cohesion,  $C_h$ , and angle of repose,  $\phi$ ), and average particle size ( $D_{50}$ ), according to ASTM standard [24]. Table 1 shows

the physical properties of six samples from the three sites of Nu'maniyah-Kut Barrage reach of Tigris Riverbanks. Strong correlations were observed between clay content and soil cohesion ( $C_h$ ) with correlation coefficient (R) of 1.00 as shown in Figure 2a. A strong relationship

between sand%, silt%, and clay% versus  $D_{50}$  with R of 0.8, 0.77, and 0.98, respectively, were reported as shown in Figure 2b. As expected, strong correlation between clay% versus  $D_{50}$  was observed.

**Table 1:** The physical properties of six samples from the three sites of Nu'maniyah-Kut Barrage reach of Tigris Riverbanks tested according to ASTM standard.

Site Number	Soil acquired	$C_h$ , kpa	$\phi$ , degree	$D_{50}$ , mm	Sand, %	Silt, %	Clay, %
1	Bank	9	31	0.18	61.6	24.4	14.0
	Toe	4	40	0.35	77.5	17.5	5.0
2	Bank	5	35	0.40	77.3	17.2	5.5
	Toe	7	42	0.25	80.2	10.8	9.0
3	Bank	6	33	0.30	77.0	16.0	7.0
	Toe	4	38	0.40	84.0	11.0	5.0

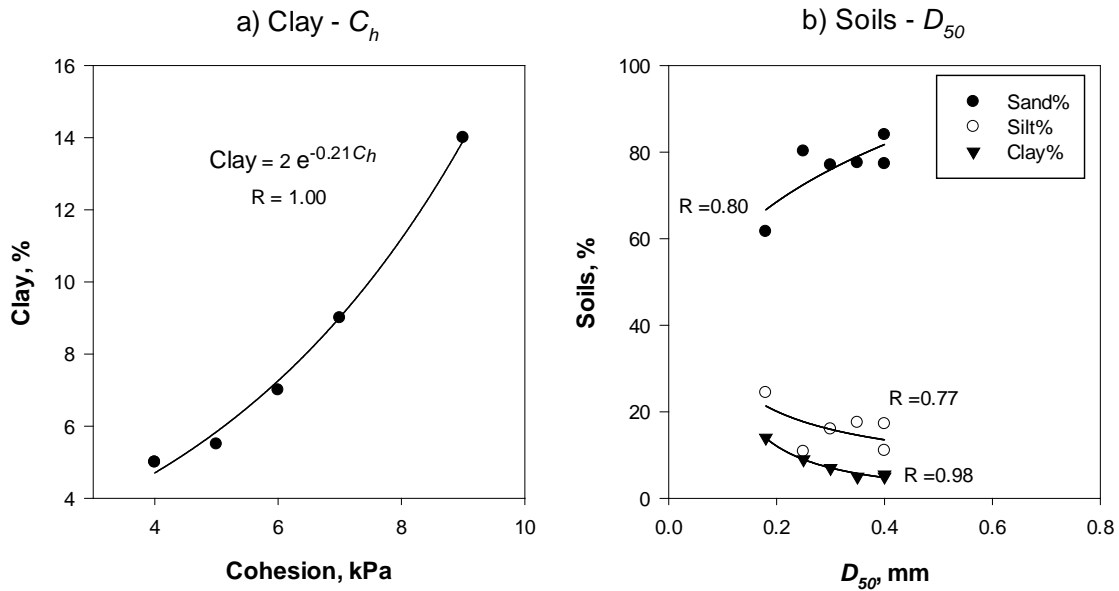


**Figure 2:** Soil physical properties relationships of six samples from the three sites of Nu'maniyah-Kut Barrage reach of Tigris Riverbanks for: a) Clay-cohesion relationship, and b) Soils- $D_{50}$  relationships.

**2.2 Laboratory “mini” JETs**

A total of 36 Jet Erosion Tests (JETs) were performed at the Hydraulic Lab of the Environmental Engineering Department, Mustansiriyah University. The “mini” JET device (Figure 3) was utilized to derive  $k_d$  and  $\tau_c$  of excess shear stress model and  $b_0$  and  $b_1$  of Wilson model. Al-Madhhachi et al. (2013a) [5] introduced the explanation, measurement, and purposes of the “mini” JET device. In this study, the coefficient discharge (C) of 0.65 was investigated and the device was standardized according to USDA and Al-Madhhachi et al. (2013a) [5].

The soil samples were first laboratory dried by air and sieved by a sieve of 4.75 mm in size

according to ASTM standard. Different quantities of water were mixed with soil samples to accomplish the selected water content, and left for 24 hr in a closed bucket to allow for moisture equilibrium. Then, soil water content of the samples was measured for each sample. The soil samples were prepared at three different water contents: dry side (3% to 5%), optimum side (13% to 14%), wet side of water content (16% to 19%), in order to investigate the variability of erodibility parameters. The compaction curves of six samples (bank and toe) at three different water contents from the three sites of Nu'maniyah-Kut Barrage reach of Tigris Riverbanks is shown in Figure 4.

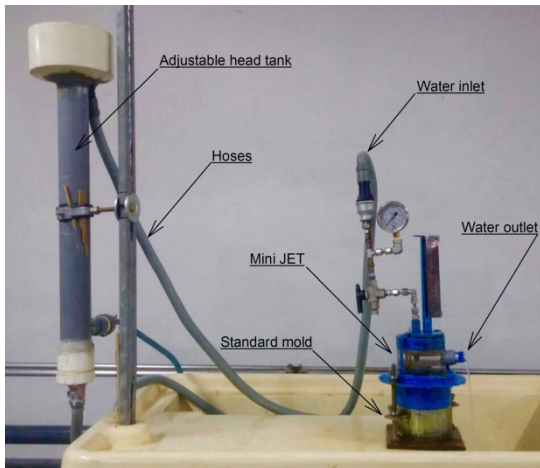


**Figure 3:** Laboratory setup of the “mini” JET device.

The ASTM standard mold (102 mm in diameter and 116 mm in height) was utilized to pack the soil samples at standard bulk density of 25 blows per layer at three layers to achieve standard bulk density at three different water contents. Accordingly, the bulk density was prepared as the one in the three field sites and it was ranged from 1.4 g/cm<sup>3</sup> to 1.8 g/cm<sup>3</sup> related to different water contents (Figure 4). A manual hammer was utilized (305 mm in height, 50.8 mm in diameter, and 2.5 kg in weight) during the packing procedure according to ASTM Standard. Then, bulk density was estimated followed by shaving the top of soil sample. After that, the soil sample was placed in centre of the submergence tank of the “mini” JET device directly below the jet nozzle (Figure 3). A water head of 70 cm for all experiments was selected. The hoses and water source were connected to the JET device. The running of JETs and collecting scour depth data versus recording time were followed Al-Madhhachi et al. (2013a) [5] and Khanal et al. (2016) [22].

**2.3 Derivation of erosion parameters**

In this study, excess shear stress model and Wilson model were used to determine soil erodibility parameters. Partheniades (1965) [3] and Hanson (1990) [4] presented the linear model based on two empirical soil parameters ( $k_d$  and  $\tau_c$ ) as following:

$$\epsilon_r = k_d (\tau - \tau_c) \tag{1}$$

where  $\epsilon_r$  is the detachment rate (cm/s), and  $\tau$  is the average hydraulic boundary shear stress (Pa), and other parameters were previously defined.

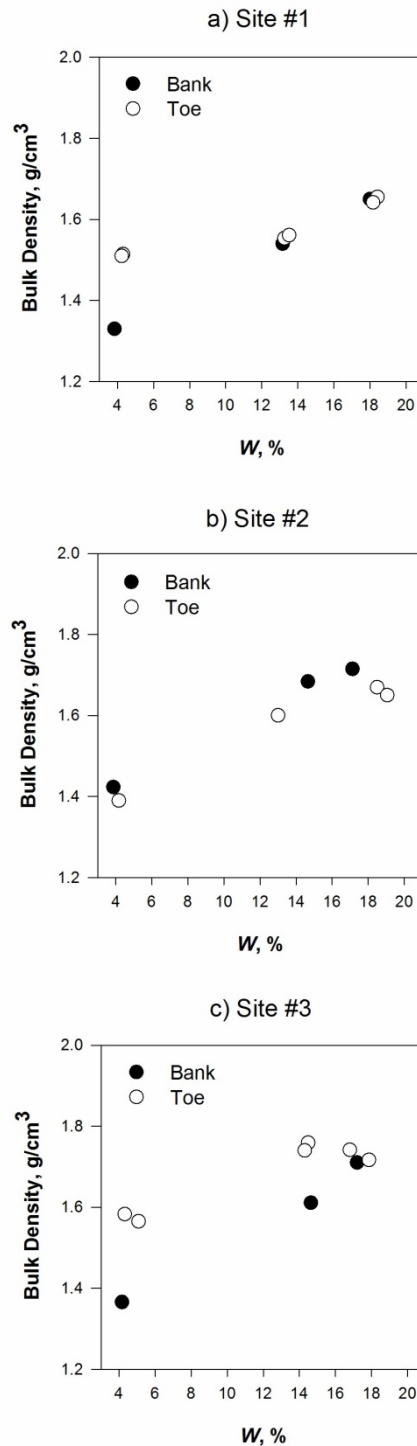


**Figure 4:** Compaction curves of six samples (bank and toe) at three different water contents from the three sites of Nu'maniyah-Kut Barrage reach of Tigris Riverbanks.

Blaisdell’s solution (BL), scour depth solution (SD), and iterative solution (IT) are recently three techniques in analyzing data from JETs to estimate the erodibility parameters of the linear model. Hanson and Cook (1997, 2004) [25, 26] developed BL solution based on Stein and Nett (1997) [27] principles theory of fluid diffusion.

Blaisdell et al. (1981) [28] developed hyperbolic function to determine equilibrium depth ( $J_e$ ) which is utilized in BL solution. The equilibrium depth ( $J_e$ ) was incorporated in  $\tau_c$  parameter based on scour depth data and it is expressed as [26]:

$$\tau_c = \tau_o \left( \frac{J_p}{J_e} \right)^2 \quad (2)$$

where  $\tau_o = C_f \rho_w U_o^2$  is the maximum shear stress due to the jet velocity at the nozzle (Pa);  $C_f = 0.00416$  is the coefficient of friction;  $\rho_w$  is water density ( $\text{kg/m}^3$ );  $U_o = C\sqrt{2gh}$  is the velocity of jet at the orifice (cm/s);  $C$  is discharge coefficient (ranged from 0.6 to 0.8 for “mini” JET);  $h$  is the pressure head (cm);  $J_p = C_d d_o$  is the potential core length from jet origin (cm);  $d_o$  is the nozzle diameter (cm); and  $C_d = 6.3$  is the diffusion constant. By solving for the least squared deviation between the observed scour time and predicted time, the  $k_d$  is then determined. The predict time is expressed as [25]:

$$T^* - T_p^* = -J^* + 0.5 \ln \left( \frac{1+J^*}{1-J^*} \right) + J_p^* - 0.5 \ln \left( \frac{1+J_p^*}{1-J_p^*} \right) \quad (3)$$

where  $T^* = t / T_r$  is the dimensional time,  $t$  is the time of a scour depth measurement,  $T_r = J_e / (k_d \tau_c)$  is the reference time according to Stein and Nett (1997) [27],  $J^* = J/J_e$ ;  $J$  is the scour depth (cm), and  $J_p^* = J_p/J_e$ .

The scour depth solution (SD) was developed by Daly et al. (2013) [14]. The SD is based on instantaneously searches for  $k_d$  and  $\tau_c$  to provide the best fit of observed scour depth data and time of JET data versus predicted curve of linear model (Eq. 1). The iterative solution (IT) was presented by Simon et al. (2010) [13]. The IT solution was modified from BL solution to improve the toughness of the solution. The erodibility parameters ( $k_d$  and  $\tau_c$ ) were initialized with values of  $k_d$  and  $\tau_c$  using BL solution. The upper bound was determined for  $\tau_c$  to prevent  $J_e$  from being exceeded. Then, a simultaneous solution to minimize the root-mean-square error between the measured and predicted time were performed to determine  $k_d$  and  $\tau_c$ . In this study, the parameters of the linear model were derived using two solution techniques: BL and SD, for JET data using Spreadsheet Tool, Version 2.1.1 that developed by Daly et al. (2013) [14], and keep away from IT solution due to unstable solution of that technique and its limitations as recommended by recent studies [18].

The Wilson model (non-linear model) is developed originally by Wilson (1993a, 1993b) [7, 8]. The model is based on removing and stabilizing forces and their moment lengths for particle soil detachment. The original framework

of the Wilson model [7, 8] was developed for open channel environment. The hydraulics of JET was incorporated by Al-Madhhachi et al. (2013b) [6] in Wilson model. Al-Madhhachi et al. (2013b) [6] verified that the Wilson model parameters can also be estimated from the experimental data obtained from the JET as following:

$$\varepsilon_r = b_0 \sqrt{\tau} \left[ 1 - \exp\{-\exp(3 - \frac{b_1}{\tau})\} \right] \quad (4)$$

where  $b_0$  is mechanistic detachment parameter ( $\text{g/m.s.N}^{0.5}$ ), and  $b_1$  is threshold parameter (Pa). In order to analyze the observed data in terms of scour depth versus time of JET data, Eq. 4 could be rewritten as:

$$\varepsilon_r = \frac{dD}{dt} = b_0 \sqrt{\tau} \left[ 1 - \exp\{-\exp(3 - \frac{b_1}{\tau})\} \right] \quad (5a)$$

which may be integrated over time for any observed scour depth data as follows:

$$D = b_0 \int_{t_0}^t \sqrt{\tau} \left[ 1 - \exp\{-\exp(3 - \frac{b_1}{\tau})\} \right] dt \quad (5b)$$

where  $D$  is scour depth at time  $t$ , and  $t_0$  is initial time. The integral form of the Eq. 5b was selected of observed scour data to decrease the sensitivity of short term fluctuations [4]. The average of observed scour data versus observed average shear stress was presented by the integral form. Equation 5b represented the series of readings (average shear stress) versus time for  $N^{\text{th}}$  shear stress and it is expressed as:

$$D = b_0 \sum_{i=1}^N \left[ \sqrt{\tau} \left[ 1 - \exp\{-\exp(3 - \frac{b_1}{\tau})\} \right] \Delta t_i \right] \quad (6)$$

The parameters  $b_0$  and  $b_1$  were determined from observed scour data versus shear stress and time. Equations 4 through 6 were incorporated in a spreadsheet tool described by Al-Madhhachi et al. (2013b) [6] to drive the Wilson parameters ( $b_0$  and  $b_1$ ) from observed JET data. Constraints were utilized within the Excel solver routine to limit potential solutions of the Wilson model parameters ( $b_0$  and  $b_1$ ) with maximum allowable variation of 50% from their initial estimated values.

### 3 Result and Discussion

A total of 36 “mini” JETs of three selected sites of Nu'maniyah-Kut Barrage reach of Tigris Riverbanks were conducted for this study under controlled laboratory setting at three different water contents ranging from 3% to 19%. Variability in derived erodibility parameters was dependent on both site properties and solution technique. Figure (5) shows the variability in derived erodibility coefficient ( $k_d$ ) of bank and toe

for three selected sites at different water contents using BL and SD solution techniques of linear model (excess shear stress model). As expected, the  $k_d$  decreased as water content increased for both solution techniques and for three sites. Lower values of  $k_d$  of toe in compares with bank side for site #1 and site #3 for both BL and SD solutions were observed especially at wet side of

water content (Figure 5a, 5b, 5e, and 5f). This was due to the influence of clay content as water content increased. While the  $k_d$  values of bank side were slightly more than the one of toe side, especially for BL solution (Figure 5c and 5d). This is due to clay content and solution technique methodology as observed in pervious researches [15, 17].

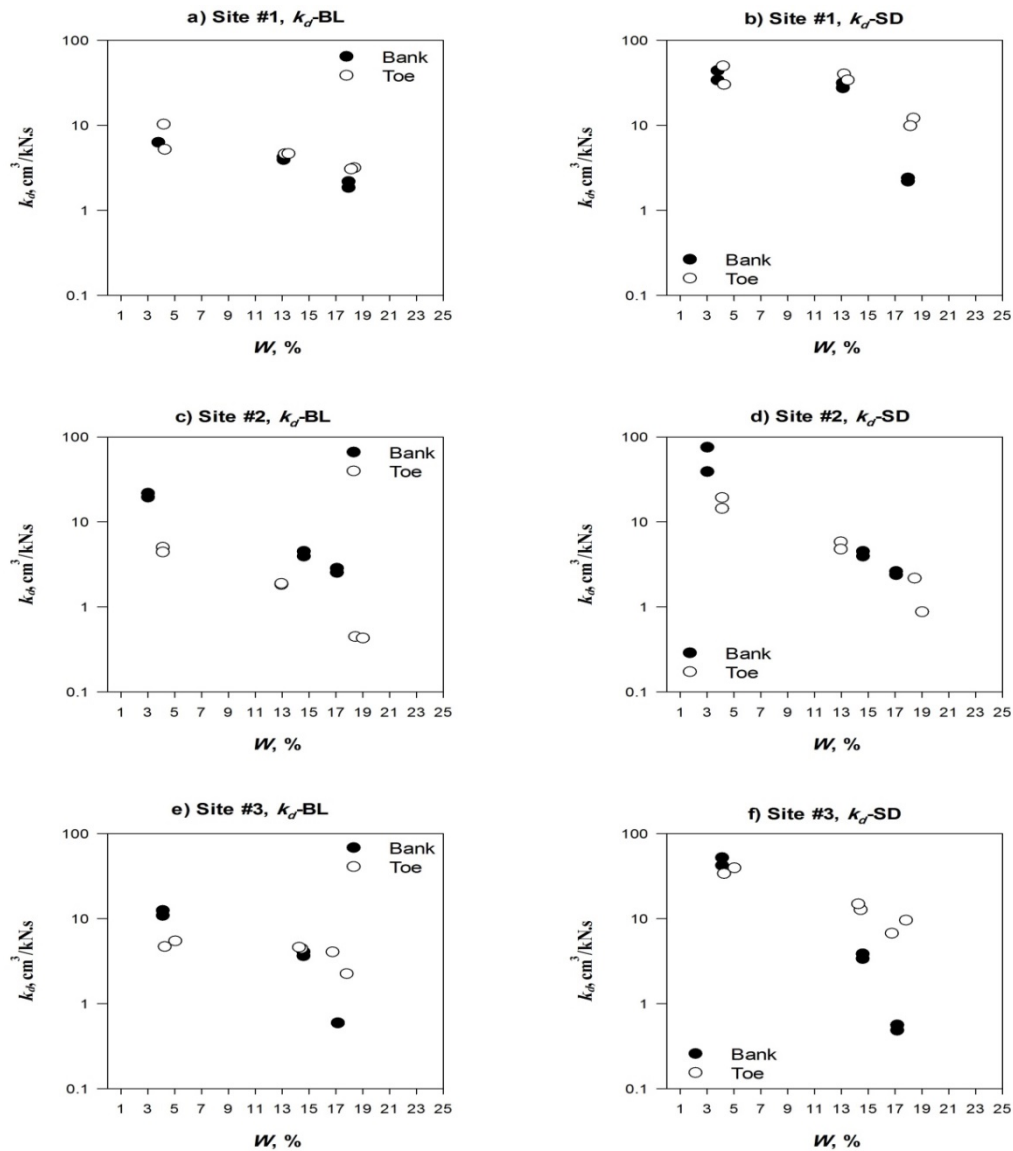


**Figure 5:** Variability in derived detachment coefficient ( $k_d$ ) of bank and toe for three selected sites of Nu'maniyah-Kut Barrage reach of Tigris Riverbanks at three different water contents using BL and SD solution techniques of linear model (excess shear stress model).

Variability in derived critical shear stress ( $\tau_c$ ) using BL and SD solution techniques of linear model (excess shear stress model) of bank and toe sides for three selected sites at three different water contents is reported in Table 2. No general pattern of  $\tau_c$  related to different water content were observed. Similar behavior was observed in other previous researches by Daly et al. (2013, 2015a, 2016) [14, 15, 17]. This was due to solution technique of both BL and SD of linear

model. A slightly increased in  $\tau_c$  values as water content increased was reported, especially for the toe side of site #2 of BL and SD solution techniques. Uncertainty solutions of some  $\tau_c$ -SD were observed due to limit potential solution of  $\tau_c$ -SD of spreadsheet tool suggested by Daly et al. (2013) [14]. Therefore, constrains are recommended in developing SD solution technique to prevent limit potential solution of  $\tau_c$ -SD in future studies.

**Table 2:** Variability in derived critical shear stress ( $\tau_c$ ) using BL and SD solution techniques of linear model (excess shear stress model) and threshold parameter ( $b_l$ ) of bank and toe sides for three selected sites of Nu'maniyah-Kut Barrage reach of Tigris Riverbanks at three different water contents.

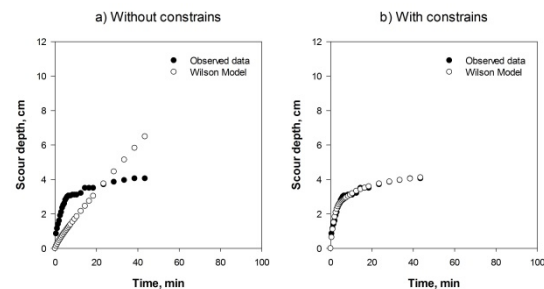
Site Number	Test #	Bank				Toe			
		W, %	$\tau_c$ -BL, Pa	$\tau_c$ -SD, Pa	$b_l$ , Pa	W, %	$\tau_c$ -BL, Pa	$\tau_c$ -SD, Pa	$b_l$ , Pa
1	1	03.8	0.180	2.040	15.97	04.3	0.080	1.700	12.64
	2	03.8	0.097	1.980	14.03	04.2	0.042	1.521	10.09
	3	13.2	0.120	1.753	13.12	13.3	0.160	1.860	14.12
	4	13.2	0.133	1.667	12.63	13.5	0.108	1.835	13.26
	5	18.0	0.029	0.064	07.28	18.4	0.070	1.819	14.44
	6	18.0	0.012	0.668	09.02	18.2	0.056	1.695	12.12
2	1	03.1	0.065	1.637	10.35	04.2	0.081	2.064	13.54
	2	03.1	0.014	1.297	08.96	04.2	0.076	2.039	13.00
	3	14.7	0.001	0.000	03.65	13.0	0.047	2.094	13.43
	4	14.7	0.002	0.264	04.85	13.0	0.024	1.898	11.97
	5	17.1	0.005	0.000	04.94	18.5	5.667	6.883	41.91
	6	17.1	0.002	0.000	03.70	19.1	5.398	6.326	39.82
3	1	04.2	0.070	1.679	11.73	05.1	0.180	2.140	15.88
	2	04.2	0.028	1.574	10.30	04.3	0.247	2.330	17.88
	3	14.6	0.001	0.000	04.66	14.5	0.020	1.460	09.15
	4	14.6	0.001	0.000	04.76	14.3	0.020	1.490	09.24
	5	17.2	0.250	0.000	00.60	17.9	0.110	2.460	13.56
	6	17.2	0.237	0.000	00.60	16.8	0.009	1.054	06.95

Similar to linear model, the uncertainty solutions for Wilson model parameters ( $b_0$  and  $b_l$ ) were observed in some tests. An example of uncertainty solutions of parameters  $b_0$  and  $b_l$  is shown in Figure 6. Figure 6a shows the solution of Wilson model without using constrains, while Figure 6b shows the solution of Wilson model with constrain. To limit potential solutions of the Wilson model parameters ( $b_0$  and  $b_l$ ), constraints were used within the Excel solver routine, as recommended by Wilson (1993b) [7] and Al-Madhhachi et al. (2013b) [6], with maximum allowable variation for the parameters ( $b_0$  and  $b_l$ ) was 50% of their initial estimated values. The Wilson model fit the data when constrain was utilized (Figure 6b).

Variability in derived  $b_0$  of bank and toe for three selected sites at three different water contents using Wilson model solution is presented in Figure 7. Similar to  $k_d$ , the  $b_0$  decreased as water content increased for three sites. The  $b_0$  followed the same behavior of  $k_d$ -SD but with different magnitude related to water contents at these sites and for bank and toe sides.

**Figure 6:** Uncertainty solutions for Wilson model parameters ( $b_0$  and  $b_l$ ) using: a) without constrains, and b) with constrains.

This fact is due to both Wilson model solution and SD solution based on same solution



technique. Similar results for different field sites were obtained from pervious researches [14, 15, 17]. Table (2) reports the variability in threshold parameter ( $b_l$ ) using Wilson model solution technique of non-linear model for bank and toe sides of three selected sites of Nu'maniyah-Kut Barrage reach of Tigris Riverbanks at three different water contents. Similar to  $\tau_c$ -SD, no general pattern of  $b_l$  related to different water content were observed. A slightly increased in  $b_l$  values as water content increased especially for the toe side of site #2. Therefore, Wilson model (non-linear model) parameters ( $b_0$  and  $b_l$ ) have the same behavior of linear model parameters ( $k_d$  and  $\tau_c$ ) but with different magnitude related to different water contents, respectively.

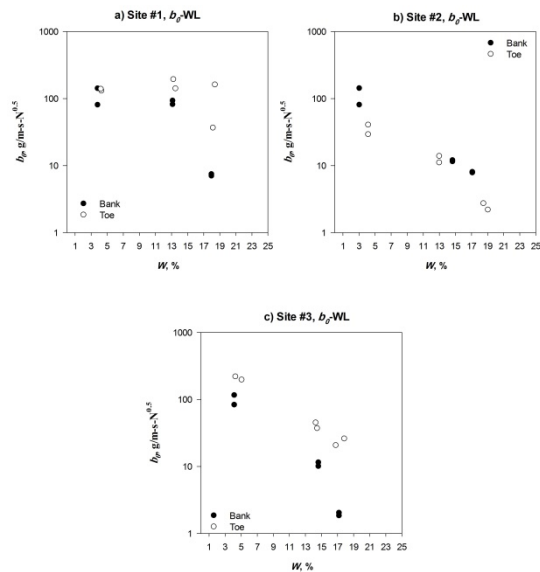
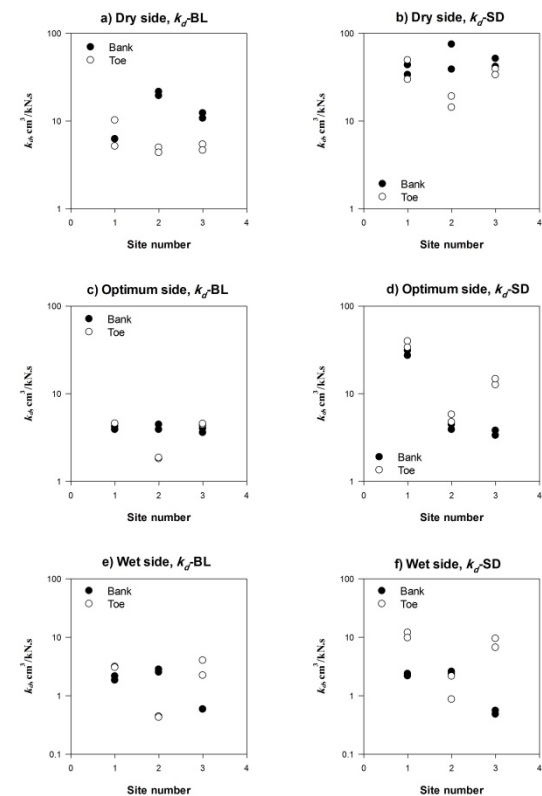


**Figure 7:** Variability in derived mechanistic detachment parameter ( $b_0$ ) of bank and toe for three selected sites of Nu'maniyah-Kut Barrage reach of Tigris Riverbanks at three different water contents using Wilson model solution (non-linear model).

The variability in derived erodibility coefficient ( $k_d$ ) of bank and toe sides related to three sites at three different water contents, using BL and SD solution techniques of linear model, were observed as shown in Figure 8. For dry side of water content, the variability of  $k_d$  for toe was less in one order than the one of bank in site #2 of both BL and SD solutions as well as in site #3 of BL solution (Figure 8a and 8b). The variability of  $k_{d-SD}$  of bank of sites #2 and #3 was less in one order than the one of site #1, while no variability were observed for  $k_{d-BL}$  at optimum water (Figure 8c and 8d). This is due to differences in solution technique between BL and SD solutions. In general, the variability of  $k_d$  increased as water contents increased due to variability in soil physical properties (especially in clay content) of these sites and between the bank and toe sides (Figure 8e and 8f). Similar behaviour was observed for  $b_0$  parameter of non-linear model (Wilson model). However, remolded soil samples in the laboratory have consistently shown much less variability comparing with performed JETs on field sites due to the influence of material heterogeneity of controlled laboratory which have much less influence on the one performed in the field sites [5, 29, 15, 17]. Therefore, investigated the correlation between soil erodibility parameters of both linear and non-linear model with soil physical properties (such as clay content and average particle size,  $D_{50}$ ) are required to understand the variability in these parameters for the three sites.

**Figure 8:** Variability in derived detachment coefficient ( $k_d$ ) of bank and toe sides related with



different three sites of Nu'maniyah-Kut Barrage reach of Tigris Riverbanks at three different water contents using BL and SD solution techniques of linear model (excess shear stress model).

The relationships between soil erodibility parameters of both linear and non-linear models and soil physical properties (clay content and  $D_{50}$ ) were reported in Figures 9 and 10. Significant correlations were observed between  $k_{d-BL}$  and clay content and  $D_{50}$  with R of 0.95 and 0.92, respectively (Figure 9a and 9c). In addition, strong correlations were observed between  $\tau_c-SD$  and clay content and  $D_{50}$  with R of 0.83 and 0.91, respectively (Figure 8b and 8d), as well as to  $\tau_c-BL$  with R of 0.93 (Figure 9d). Note that, the values of  $k_{d-SD}$  are parallel to  $k_{d-BL}$  with one order larger related to clay content and  $D_{50}$  (Figure 9a and 9c).

No significant correlations were observed between ( $b_0$  and  $b_1$ ) of Wilson model and clay content and  $D_{50}$  were observed except the relation between  $b_1$  and  $D_{50}$  with R of 0.91 (Figure 10). Daly et al. (2015a) [15] reported no significant correlations were observed between erodibility parameters and soil physical properties. This is due to the effected of soil heterogeneity of JETs in the field comparing to the one in the laboratory. Therefore, performing wide range testing of JETs on wide range sites of Nu'maniyah-Kut Barrage reach of Tigris Riverbanks is recommended for future studies in order to drive more correct correlations between soil erodibility parameters of both linear and non-linear models and soil physical properties.



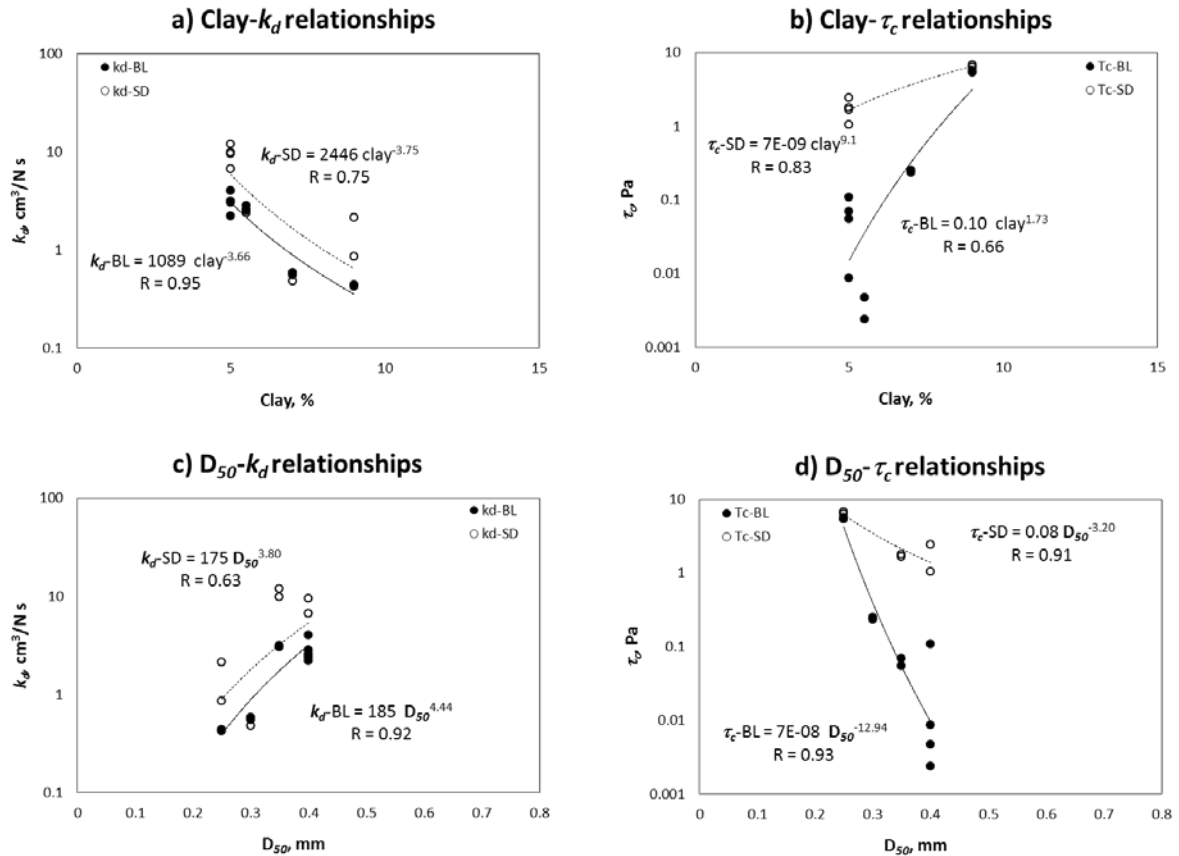


**Figure 9:** Relationships between linear model parameters ( $k_d$  and  $\tau_c$ ) and soil physical properties (Clay% and  $D_{50}$ ) of both BL and SD solutions of Nu'maniyah-Kut Barrage reach of Tigris Riverbanks sites.

#### 4 Conclusions

JETs are usually utilized to determine linear model parameters ( $k_d$  and  $\tau_c$ ) as well as a non-linear model parameters ( $b_0$  and  $b_1$ ). Two solutions (BL and SD) of excess shear stress model (linear model) were performed. Note that Wilson model (non-linear model) solution and SD solution based on same concept and same solution technique. A case study of three sites of Nu'maniyah-Kut Barrage reach of Tigris Riverbanks were performed to investigate the variability of soil erodibility parameters ( $k_d$ ,  $\tau_c$ ,  $b_0$ , and  $b_1$ ) at the three different water contents as well as to perform relationships of these parameters with soil physical properties.

The results from JETs at three sites showed less variability of soil erodibility parameters compared with previous studies performed on field sites. This is due to the influence of material heterogeneity in controlled laboratory compared with the performed one in the field sites. This

study reported similarities between linear and non-linear model parameters behavior related to different water contents but different magnitude, with a benefit of mechanistic parameters of Wilson model. Strong correlations ( $R$  of 0.83 to 0.95) were observed between  $k_d$ -BL,  $\tau_c$ -BL,  $\tau_c$ -SD with clay content as well as to  $D_{50}$ , respectively. Parallel values of  $k_d$ -SD versus  $k_d$ -BL were observed with one order larger related to clay content and  $D_{50}$ . No significant correlations were observed between ( $b_0$  and  $b_1$ ) of Wilson model and clay content and  $D_{50}$ , expected the relation between  $b_1$  and  $D_{50}$ . This study recommended of performing wide testing range of JETs on wide range sites of Nu'maniyah-Kut Barrage reach of Tigris Riverbanks for future studies in order to drive more appropriate correlations between soil erodibility parameters of both linear and non-linear models and soil physical properties.

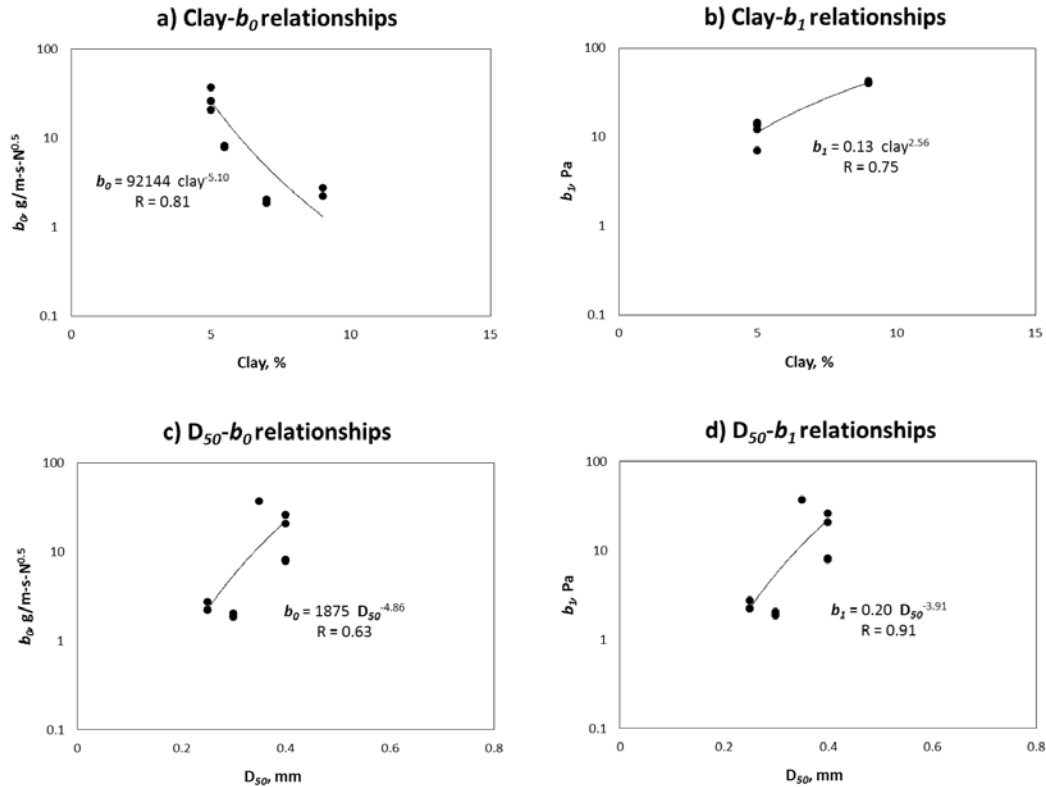


**Figure 10:** Relationships between non-linear model (Wilson model) parameters ( $b_0$  and  $b_1$ ) and soil physical properties (Clay% and  $D_{50}$ ) of Nu'maniyah-Kut Barrage reach of Tigris Riverbanks sites.

**5 References**

[1] Simon, A., Curini, A., Darby, S. E., and Langendoen, E. J. (2000). Bank and near bank processes in an incised channel. *Geomorphology*, 35 (3-4): 193-217.

[2] Fox, G.A., and Wilson, G.V. (2010). The role of subsurface flow in hillslope and stream bank erosion: a review. *Soil Sci. Soc.Am.J.*,74(1),717-733. <http://dx.doi.org/10.2135/sssaj2009.0319>.

[3] Partheniades, E. (1965). Erosion and deposition of cohesive soils. *J. Hydraul. Div., ASCE*, 91(1), 105-139.

[4] Hanson, G. J. (1990). Surface erodibility of earthen channels at high stresses. II: Developing an in situ testing device. *T. ASAE*, 33(1): 132-137.

[5] Al-Madhhachi, A. T., Hanson, G. J., Fox, G. A., Tyagi, A. K., and Bulut, R. (2013a). Measuring soil erodibility using a laboratory “mini” JET. *Trans. ASABE*, 56(3), 901-910. DOI: 10.1061/41173(414) 244.

[6] Al-Madhhachi, A. T., Hanson, G. J., Fox, G. A., Tyagi, A. K., and Bulut, R. (2013b). Deriving parameters of a fundamental detachment model for cohesive soils from flume and jet erosion tests. *Trans. ASABE*, 56(2), 489-504. DOI: 10.13031/2013. 42669.

[7] Wilson, B. N. (1993a). Development of a fundamental based detachment model. *Transaction of ASAE*, 36(4): 1105-1114.

[8] Wilson, B. N. (1993b). Evaluation of a fundamental based detachment model. *Transaction of ASAE*, 36(4): 1115-1122.

[9] Hanson, G. J., and Hunt, S. (2007). Lessons learned using laboratory JET method to measure soil erodibility of compacted soils. *Appl. Eng. Agr.*, 23(3), 305-312. DOI: 10.13031/2013.22686.

[10] Clark, L.A., and Wynn, T.M. (2007). Methods for determining streambank critical shear stress and soil erodibility: implications for erosion rate predictions. *Transaction of ASABE*, 50(1), 95-106. Doi.org/10.13031/2013.22415.

[11] Utley, B., and Wynn, T. (2008). Cohesive soil erosion: theory and practice. *World Environmental and Water Resources Congress*, 2008, pp.1-10.

[12] Hanson, G. J., and Simon, A. (2001). Erodibility of cohesive streambeds in the loess area of the midwestern USA. *Hydrological processes*, 15(1), 23-38. DOI: 10.1002/hyp.149.

[13] Simon, A., Thomas, R., and Klimetz, L. (2010). Comparison and experiences with field techniques to measure critical shear stress and erodibility of cohesive deposits. Proc., 2nd Joint Federal Interagency Conference, Las Vegas, NV.

[14] Daly, E. R., Fox, G. A., Al-Madhhachi, A. T., and Miller, R. (2013). A scour depth approach for deriving erodibility parameters from Jet Erosion Tests. *Trans. ASABE*, 56(6), 1343-1351. DOI: 10.13031/trans.56.10350.

- [15] Daly, E. R., Fox, G. A., Al-Madhhachi, A. T., and Storm, D. E. (2015a). Variability of fluvial erodibility parameters for streambanks on a watershed scale. *Geomorphology*, 231, 281-291. DOI:10.1016/j.geomorph.2014.12.016.
- [16] Daly, E., Miller, R. B., and Fox, G. A. (2015b). Modeling streambank erosion and failure along protected and unprotected composite streambanks. *Advances in Water Resources*, 81, 114-127.
- [17] Daly, E. R., Fox, G. A., and Fox, A. K. (2016). Correlating site-scale erodibility parameters from jet erosion tests to soil physical properties. *Trans. ASABE*, 59(1): 115-128. DOI 10.13031/trans.59.11309.
- [18] Salah, M., and Al-Madhhachi, A. T. (2016). Influence of Lead Pollution on Cohesive Soil Erodibility using Jet Erosion Tests. *Environment and Natural Resources Research*; Vol. 6(1): 88-98.
- [19] Langendoen, E. J. (2000). CONCEPTS — conservational channel evolution and pollutant transport system, stream corridor version 1.0. U.S. Department of Agriculture, Agricultural Research Service, Oxford, MS.
- [20] Ulrich, J. S., and Nieber, J. L. (2008). Streambank and bluff erosion modeling for the Knife River, Minnesota. ASABE Paper No. 084478. ASABE, St. Joseph, MI <http://dx.doi.org/10.13031/2013.25072>.
- [21] Midgley, T. L., Fox, G. A., and Heeren, D. M. (2012). Evaluation of the bank stability and toe erosion model (BSTEM) for predicting lateral streambank retreat on composite streambanks. *Geomorphology*; 145–146:107–14.
- [22] Khanal, A., Fox, G. A., and Al-Madhhachi, A. T. (2016). Variability of erodibility parameters from laboratory mini Jet Erosion Tests. *Journal of Hydrologic Engineering, ASCE*, ISSN 1084-0699/ 04016030-1.
- [23] Abdul-Sahib, A. A. (2014). *Roughness Characteristics of The Kut-Nu'maniyah reach of the Tigris River and Its Effect on Nu'maniyah Gaging Station*. M.Sc. Thesis, Baghdad University, Baghdad, Iraq.
- [24] ASTM Standards. (2006). Section 4: Construction. In *Annual Book of ASTM Standards*. Philadelphia, Pa.: ASTM.
- [25] Hanson, G. J., and Cook, K. (1997). Development of excess shear stress parameters for circular jet testing. ASAE Paper, 972227. St. Joseph, Mich: ASAE.
- [26] Hanson, G. J., and Cook, K. (2004). Apparatus, test procedures, and analytical methods to measure soil erodibility in situ. *Appl. Eng. Agr.*, 20(4), 455-462. DOI: 10.13031/2013.16492.
- [27] Stein, O. R., and Nett, D. D. (1997). Impinging jet calibration of excess shear sediment detachment parameters. *Trans. ASAE*, 40(6): 1573-1580. DOI: 10.13031/2013.21421.
- [28] Blaisdell, F. W., Clayton, L. A., and Hebaus, C. G. (1981). Ultimate dimension of local scour. *J. Hydraulics Division, ASCE*, 107(HY3): 327-337.
- [29] Layzell, A. L., and Mandel, R. D. (2014). An assessment of the erodibility of Holocene lithounits comprising streambanks in northeastern Kansas, USA. *Geomorphology*, 213, 116–127.

## التغيرات في معاملات تعريه التربة لضفاف نهر دجلة باستخدام الموديل الخطي و الغير خطي

عبدالصاحب توفيق المذحجي

قسم هندسة البيئه – كلية الهندسه  
الجامعه المستنصريه

### الخلاصة

يتم في اغلب البحوث حساب تآكل التربة من ضفاف الانهر الممتاسكه باستخدام النموذج الخطي (معادله إجهاد القص الفائض) و نموذج غير الخطي (نموذج ويلسون) بالاعتماد على معاملتين للتربة (معامل التعريه,  $K_d$  وإجهاد قص الحرج,  $\tau_c$ ) بالنسبه للنموذج الخطي و بالاعتماد على معاملتين ميكانيكيتين للتربة (معامل التعريه الميكانيكي,  $b_0$  و معامل القص,  $b_1$ ). الهدف من هذا البحث هو قياس تعريه التربة لضفاف نهر دجلة في المنطقه المحصوره بين النعمانية و سدة الكوت باستخدام النموذجين الخطي والغير الخطي من خلال معاملات النموذجين لثلاث محتويات رطوبة للتربة: الجانب الجاف، الجانب الأمتل، والجانب الرطب من محتوى الرطوبي للتربة. عينات التربة تم جمعها من ثلاثة مواقع في جنوب بغداد للمنطقه الواقعه بين النعمانية و سدة الكوت على ضفاف نهر دجلة. ست عينات من التربة تم الحصول عليها من هذه المواقع و تم فحصها و اختبارها مختبريا باستخدام نسخة مصغرة من جهاز جيت ("mini" JET) للحصول على معاملات التعريه للنموذجين الخطي والغير الخطي. طريقه Blaisdell (BL) وطريقه عمق التاكل (SD) قد استخدمت لإيجاد معاملات التعريه ( $K_d$  and  $\tau_c$ ) للنموذج الخطي من بيانات جهاز JET. خصائص التربة الفيزيائية و تشمل: الكثافة، نسبه جسيمات التربة (الرمال، الطمي، والطين)، متوسط حجم الجسيمات ( $D_{50}$ )، و زاوية الاحتكاك قد تم حسابهم للعينات الستة من المواقع الثلاثة. أظهرت النتائج انخفاض في قيم  $K_d$  في أسفل ضفه النهر بالمقارنة مع الجانب العلوي من هذه المواقع لكل من الطرقتين BL و SD المحسوبه من معادله إجهاد قص الفائض وخصوصا في الجانب الرطب من محتوى الرطوبي للتربة. لم يتم ملاحظه أي نمط عام بالنسبه للمعامل  $\tau_c$  على مختلف المحتوى الرطوبي للتربة. المعاملات ( $b_0$  and  $b_1$ ) من نموذج الغير الخطي لها نفس سلوك المعاملات ( $K_d$  and  $\tau_c$ ) من نموذج الخطي ولكن مختلفه في القيم بالنسبه لمختلف المحتوى الرطوبي للتربة.